RSC Advances

PAPER

View Article Online
View Journal | View Issue

Open Access Article. Published on 22 September 2021. Downloaded on 11/11/2025 4:36:28 PM.
This article is licensed under a Creative Commons Attribution-NonCommercial 3.0 Unported Licence.

Check for updates

Cite this: *RSC Adv.*, 2021, **11**, 31364

Effect of applied voltage on membrane fouling in the amplifying anaerobic electrochemical membrane bioreactor for long-term operation†

Mengjing Cao,[ab] Yongxiang Zhang[ab] and Yan Zhang *[ab]

A novel and amplifying anaerobic electrochemical membrane bioreactor (AnEMBR, R2) was constructed and operated for a long time (204 days) with synthetic glucose solution having an average chemical oxygen demand (COD) of 315 mg L^{-1}, at different applied voltages and room temperatures. More than twice sodium bicarbonate was added for maintaining a pH of around 6.7 in the supernatant of the reactor R2, close to that of a control reactor called anaerobic membrane bioreactor (AnMBR, R1), after 138 days. And the transmembrane pressure (TMP) for the R2 system was only 0.534 bar at the end of operation and 0.615 bar for the R1 system. Although the electrostatic repulsion force contributed to pushing away the pollutants (proteins, polysaccharose and inorganic salt deposits, and so on), more microorganisms adsorbed and accumulated on the membrane surface after the whole operation, which might result in a rapid increase in membrane filtration resistance in the long-term operation. There were much more exoelectrogenic bacteria, mainly Betaproteobacteria, Deltaproteobacteria and Grammaproteobacteria, on the cathode and the dominant methanogen *Methanothrix* content on the cathode was three times higher than the AnMBR. The study provides an important theoretical foundation for the application of AnEMBR technology in the treatment of low organic strength wastewater.

Received 18th July 2021
Accepted 2nd September 2021

DOI: 10.1039/d1ra05500c

rsc.li/rsc-advances

1. Introduction

Anaerobic membrane bioreactor (AnMBR) technology for domestic wastewater treatment has been studied increasingly due to producing value-added products, solid free effluent and occupying a small footprint.[1–5] However, membrane fouling in the AnMBR has already been a considerable setback in real engineering application.[6] The main factors causing membrane fouling are organic pollutants, inorganic pollutants and microbial pollutants, which originate mainly from the active sludge.[7,8] Furthermore, extracellular polymeric substances (EPS) and soluble microbial products (SMP)[9] produced by microorganisms were the main reason for membrane fouling. The polymeric compounds in the active sludge were correlated positively to the negative surface charges of active sludge flocs.[10] And the increased negative surface charges in the sludge flocs would contribute to stronger repulsive electrostatic interactions and weaker bonding among different particles.[11] And this means that it is an effective way to suppress membrane fouling and increase membrane service life by changing the surface property of the sludge flocs.

Integrating microbial fuel cell (MFC) with AnMBR has been proved to be an effective fouling control strategy by reducing particle zeta potential and the amount of SMP in the cathodic mixed liquor.[12] But there are two main difficulties for wide application of the MFC system. On one hand, it is difficult to remain the same power densities in the practical engineering application as that in the laboratory system.[13] On the other hand, the stability of large bioelectrochemical systems is poor for a long-term operation.[13] These problems have been turned out to be closely related to the cathode inevitable biofilm.[14] The biofilm growth resulted in increasing fouling of the cathode outer surface.[15] And salt deposition, humic acid adsorption and microbial by-products were formed into internal pollutants on the cathode.[16–18] Fortunately, a novel anaerobic electrochemical membrane bioreactor (AnEMBR) was developed by Katuri *et al.* firstly.[19] The stability of cathode was enhanced strongly by regulating the applied voltage and the membrane biofouling was mitigated, which could be due to a combination of factors (hydrogen bubble formation, low cathode potential and pH) in this system.[19] But there are many problems to be solved in the AnEMBR research filed now.

Metal materials were usually adopted directly as the cathode unit, not environment-friendly products.[19,20] Katuri *et al.* incorporated an electrically conductive nickel-based hollow fiber membrane (Ni-HFM) as the basic separation unit in an

[a]*Faculty of Architecture, Civil and Transportation Engineering, Beijing University of Technology, Beijing 100124, China. E-mail: yzhang@bjut.edu.cn; Tel: +86 13693219897*

[b]*Key Laboratory of Beijing for Water Quality Science and Water Environment Recovery Engineering, Beijing University of Technology, Beijing 100124, China*

† Electronic supplementary information (ESI) available. See DOI: 10.1039/d1ra05500c

© 2021 The Author(s). Published by the Royal Society of Chemistry

Open Access Article. Published on 22 September 2021. Downloaded on 11/11/2025 4:36:28 PM. This article is licensed under a Creative Commons Attribution-NonCommercial 3.0 Unported Licence.

AnEMBR system.[19] But metal ions in metal membrane might flow into the water through hydraulic-action or ion-exchange and result in potential environmental risk.[21] The physical, chemical and biological properties of sludge on the membrane surface may be changed by applied voltage.[22,23]

The conductive hollow fiber membrane prepared by carbon nanotubes as a basic separation and cathode overcame above problems.[21] The good performance of the carbon nanotubes hollow fiber membrane was attributed to high mechanical strength, good hydrophilic characteristics, large specific surface area and encouraging electrical conductivity of carbon nanotubes.[24] And Yang *et al.* found that the carbon nanotubes hollow fiber membrane with negative electro-assistance mitigated membrane pore blocking in the AnEMBR.[21] There are two main reasons to suppress the membrane fouling in the AnEMBR system. Increased biogas was produced on the membrane surface, which was similar to a weak gas sparging; less pollutants, especially EPS, were adsorbed and accumulated on the membrane surface because of like electrostatic repulsion between conductive membrane surface and active sludge. But the current studies about the AnEMBR system mainly stay in laboratory-scale system, and with small size. Namely, the reactors were usually small, had a working volume of <1 L or 1 L, and the reactors were operated for <100 days.[19,21,25] Hence, it is necessary to explore the performance and membrane fouling control mechanisms of the larger AnEMBR system for a long-term operation, especially, to observe the complicated relationship between the applied voltage and the increased rate of membrane fouling, and compare the differences with the small AnEMBR system.

To address these objectives, an amplifying anaerobic electrochemical membrane bioreactor (AnEMBR) was constructed firstly by the modified polyvinylidene fluoride (PVDF) hollow fiber membrane by coating with multiwalled carbon nanotubes (HF-PVDF-CNT) as the basic separation unit and cathode simultaneously. The operation conditions (pH, temperature, oxidation–reduction potential, and dissolved oxygen) were online monitored to analyze the specific factors and conditions during the whole long-term experiment. The membrane fouling propensity was detected continuously in terms of transmembrane pressure (TMP). The organic, inorganic and physicochemical characteristics, CH_4 production and microbial communities were observed for exploring antifouling mechanism in a long-term operation, especially analyzing the difference with the small AnEMBR system.

2. Materials and methods

2.1 AnEMBR setup and operation

An amplifying anaerobic electrochemical membrane bioreactor (R2 system) with 3.2 L of working volume (50 cm height, 9.4 cm internal diameter) was run at room temperatures in a continuous upflow mode for 204 days. The hydraulic retention time (HRT) of the reactor was about 36 h. HF-PVDF-CNT membranes were used as the basic separation unit of the reactor R2. HF-PVDF-CNT membranes were fabricated by filtration coating, and the prepared procedures in detail were the same as our previous research.[26] The experimental bioreactor setup is shown in Fig. S1,† similar to the AnEMBR setup constructed by Katuri *et al.*[19] But in our AnEMBR system, the cylindrical carbon-graphite felt containing a platinum core adhered strongly anaerobic sludge was used as the anode, and the HF-PVDF-CNT membrane module (contained HF-PVDF-CNT 10 membrane wires) was used as cathode. Bottom radius and height of the carbon-graphite felt were 8 cm and 10 cm, respectively. The working area of the membrane module was 351.68 cm^2. The vertical distance between the end of cathode and the top of the anode was about 5 cm. There were many on-line monitoring devices on the top of the reactor R2 to monitor the parameters, including pH, temperature (T), oxidation–reduction potential (ORP), and dissolved oxygen (DO). The electrochemical workstation (CORRTEST, Wuhan, China) was placed between anode and cathode to measure potentials, and provided stable negative potentials for the cathode. Other parameters are presented in the ESI (Tables S1–S4†). An anaerobic membrane bioreactor (AnMBR, R1), similar to the R2 system, was operated in parallel under the same environmental conditions, except there was no applied voltage on the membrane surface and no carbon-graphite felt existed in the sludge zone. Both systems were inoculated with anaerobic sludge from the secondary sedimentation tank of Beijing Gaobeidian sewage treatment plant. The sludge concentration (MLSS) in both reactors after inoculation was 3000 mg L^{-1}.

2.2 Measuring method

The chemical oxygen demand (COD) concentrations were determined by standard methods.[27] The morphologies on the membrane surface were observed by scanning electron microscopy (SEM, SU8020, Japan). The transmembrane pressure (TMP) of membrane modules was monitored by the pressure transducer (JYB-3151, Beijing, China). The chemical component of pollutants on the membrane surface was detected by Attenuated Total Reflection (ATR)-Fourier infrared spectrometer (FTIR, Nicolet iS10, USA). Three-dimensional excitation emission matrix (3D EEM) fluorescence spectroscopy (F-7000, Hitachi, Japan) was used to determine the composition in EPS of sludge after stimulation by voltage. The fluorescence spectrometer (XRF, SRS3400, Germany) was used to analyze inorganic elements of pollutants on the membrane surface. The chemical component of pollutants, zeta potential, particle size of sludge, and mixed gas composition were detected in Zhongke Baice Technology Service Co., Ltd (Beijing, China). High-throughput sequencing technologies were used to investigate the microbial community change under an electrochemical environment. The detailed procedures are presented in the ESI.†

3. Results and discussion

3.1 Experiment factors

The reactors R1 and R2 were operated continuously at room temperatures. The temperatures of internal mixed solutions for two reactors remained equal or close at all times, as illustrated

Open Access Article. Published on 22 September 2021. Downloaded on 11/11/2025 4:36:28 PM.
This article is licensed under a Creative Commons Attribution-NonCommercial 3.0 Unported Licence.

in the Fig. S2.† And the oxidation–reduction potential (ORP) evolution profiles during the operation (204 days) were obtained to evaluate the oxygen concentration in the solutions.[28] As shown in Fig. S3,† the initial ORPs for the reactors R1, R2 were −295 and −301 mV, respectively. Methanogens were not fit for living in the condition. This could be a reflection of low anaerobic microbial activity in the initial environment. And the ORP growth rate of R2 system was lower than that of R1 system. The ORP tended to be stable up to 42 days in the reactor R1, but up to 50 days in the reactor R2. It may suggest that the cathode potential (−0.5 V) was not optimal.

Moreover, the supernatant pH values remained relatively stable following adding a quantitative $NaHCO_3$ during the whole operation in the reactor R1 (Fig. 1), even tended to increase slightly. In the reactor R2, initial buffered medium contained the same compositions as the reactor R1. But the serious acidification was in the presence of the reactor R2 at 100 days. The supernatant pH values decreased rapidly within 100–114 days, and stabilized at a lower level within 115–125 days. The supernatant in the AnEMBR (R2) acted for liquor in the cathode chamber of the microbial electrolysis cell (MEC). So, acidification could be caused by the accumulation of excess protons produced by microbial metabolism in the anode zone. The protons were not consumed absolutely in time in the anode or cathode zone (mainly cathode zone). It suggests that the protons utilization was low on the conductive cathode membrane because the probe of pH online detector was placed near the cathode. And carbonates and phosphates with low concentrations, had a weak pH buffering capacity. To improve the performance deterioration, the concentration of $NaHCO_3$ in influent of the reactor R2 increased from 0.3 g L^{-1} to 0.5 g L^{-1} at 125 days, 0.7 g L^{-1} at 138 days, respectively. With the increase of $NaHCO_3$, the pH increased gradually from 6.2 to 6.7 in the supernatant of AnEMBR system up to 143 days. In general, the optimal pH range was 6.5–7.5 for methanogens living. Obviously, pH value was in the optimal pH range for the reactor R2 after 143 days. And difference of pH values was <0.2 between two reactors at the same point in time during the whole operation, except when the reactor R2 broke down. It suggests that higher alkalinity could prevent the AnEMBR system from acidification. It is necessary to make an additional cost to ensure the AnEMBR system operation for a long time, due to an increase in the alkalinity demand, compared with the AnMBR system. This was an important and different factor for the long-running AnEMBR system, compared with the short-running AnEMBR system.

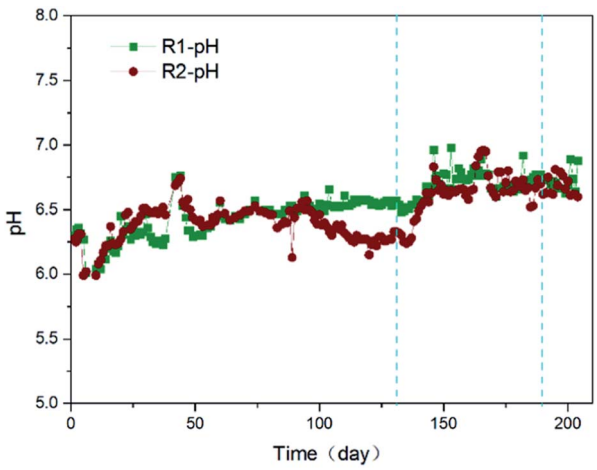

Fig. 1 pH of the supernatant during the whole operation of the reactors R1 and R2.

3.2 COD removal performance

The COD removal of both anaerobic membrane bioreactors (R1 and R2) is illustrated in Fig. 2(a). And the colour of two reactors changed gradually, as shown in Fig. 2(c)–(f). The surface potentials on the cathode in the reactor R2 were kept stable at different stages (Table S4†). Influent COD concentrations were highly volatile in the first 20 days. It could be attributed to the reasons that glucose was easy to be converted into volatile fatty acids (VFAs) naturally in the long-placed raw solution, which could lead to the changes of influent COD concentration. But COD concentration in the raw solution was stable at around 315 mg L^{-1} by shortening storage period after 40 days. Although pH of the supernatant had changed in the reactor R2 by increasing the influent pH values (controlled by $NaHCO_3$) after 125 days, the COD concentrations were very close between each other and both average influent COD concentrations were always about 315 mg L^{-1}.

As is shown in the Fig. 2(b), the COD removal changes were similar between each other before 65 days. COD concentrations in effluent decreased in the first 8 days and increased within 9–21 days. This may be for the reasons that anaerobic microorganisms had to take some time to adopt the new environment for growing and enriching, while initial organic matter in the inoculated sludge from the wastewater treatment plant was to be digested and diluted with replaced tap water. COD concentrations in effluent were relatively high from 8 to 65 days, but declined gradually. It may suggest that a lot of bacteria died and dominant population was too low to digest excess organic matter, but the dominant bacteria was enriching. There was some difference for COD removal in both reactors. The effluent COD concentration was stable at a low level in the reactor R1 after 66 days. But the low and stable COD concentration only existed within 66–110 days when the cathode potential was −0.5 V in the reactor R2. The COD concentration in effluent showed a liner rate of increase from the 110 days to 123 days during the operation of R2 system. Surprisingly, the COD concentration in effluent at 123 days had already been more than that at the first day in the reactor R2. There was little or no biological activity in the R2 system at 123 days. At the same time, the system R2 was examined from head to toe within 13 days. pH values in supernatant of the reactor R2 (6.15–6.35) were lower than those in supernatant of the reactor R1 (6.5–6.6) within 110–123 days, and the pH began to decrease at 100 days. It could be seen that R2 system exhibited a poor self-regulating ability for acidification in the long-term operation, compared with R1 system. So, the concentration of $NaHCO_3$ in influent of

 © 2021 The Author(s). Published by the Royal Society of Chemistry

Open Access Article. Published on 22 September 2021. Downloaded on 11/11/2025 4:36:28 PM.
This article is licensed under a Creative Commons Attribution-NonCommercial 3.0 Unported Licence.

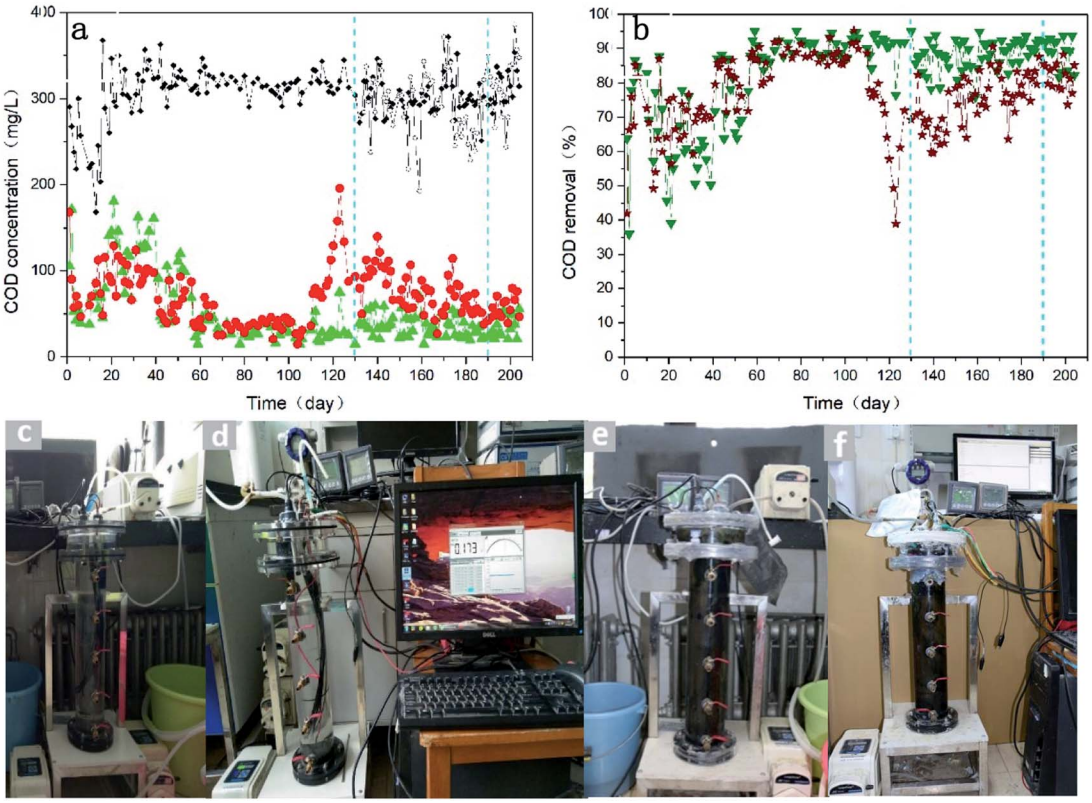

Fig. 2 COD removal during the whole operation of the reactors R1 and R2 (a) and (b). Physical diagram of R1 (c) and R2 (d) before operation. Physical diagram of R1 (e) and R2 (f) under operation.

the reactor R2 increased from 0.3 g L^{-1} to 0.5 g L^{-1} at 125 days. Interestingly, effluent COD concentration decreased rapidly in the reactor R2 during two days. But effluent COD concentration maintained relatively high level and the optimal anaerobic environment was still not be absolutely recovered in the reactor R2 up to 138 days. For better comparative analysis, the concentration of $NaHCO_3$ in influent of the reactor R2 continued to be increased by 0.2 g L^{-1} and the corresponding pH is 6.5 in the supernatant at 138 days. The pH value was approximate to that in the supernatant of the reactor R1. However, there was no better COD removal than that of the reactor R1.

Furthermore, the average COD concentration was 33.68 mg L^{-1} in effluent of the reactor R1 during the stable operation. And the average COD concentrations in effluent of the reactor R2 from stage 1 to 3 were 37.79, 64.20 and 39.62 mg L^{-1}, respectively. As shown in Fig. S4 (left),† there was obvious difference for SCOD concentrations in both supernatants. The average SCOD concentration was 57.09 mg L^{-1} in supernatant of the reactor R1 during the stable operation. But average SCOD concentrations in supernatant of the reactor R2 from stage 1–3 in order were 67.48, 105.09 and 98.51 mg L^{-1}, respectively. Both average COD concentration in influent of the reactors R1 and R2 was 315 mg L^{-1}. So, the biological treatment contribution rate and membrane separation contribution rate of R1 and R2 were 91.68% and 8.32%, respectively. It could be seen that anaerobic digestion process in the system R1 played a major role for treatment of synthetic wastewater. Glucose as a simple organic compound, finally was converted smoothly into methane, hydrogen and carbon dioxide through anaerobic digestion process in the R1 system. In comparison, biological treatment contribution rates of the reactor R2 from stage 1 to 3 were 89.29%, 83.70% and 83.38%, respectively. Membrane separation contribution rates in supernatant of the reactor R2 from stage 1 to 3 were 10.71%, 16.30% and 16.62%, respectively. Obviously, membrane separation contribution rates of the reactor R2 were all higher than that of the reactor R1, but the trend for biological treatment contribution in sludge zone was opposite. It could suggest that the applied voltage had a positive effect on organic degradation or repulsion in the cathode zone, but a negative relatively effect on organic degradation in the anode zone. And it might be attributed to the electrostatic repulsion enhancing the membrane separation. If the biological treatment efficiency had been improved, the transfer velocity of electrons and protons would be a key factor, especially for the large reactors. And the control of alkalinity would be an important and effective way to solve the problem of acidification in the AnEMBR system. Hence, it is important to research the effect of different pH on the AnEMBR system and seek optimal solutions to accelerate the transfer of electrons and protons in the future.

In addition, acetate was the major component of the volatile fatty acids in the supernatant of both reactors (Fig. S4 (right)†). The acetate concentrations in the supernatant of the reactor R2

Open Access Article. Published on 22 September 2021. Downloaded on 11/11/2025 4:36:28 PM.
This article is licensed under a Creative Commons Attribution-NonCommercial 3.0 Unported Licence.

(8.18, 18.91 and 22.48 mg L^{-1}, from the stage 1 to 3, respectively), were always more than those in the reactor R1 (6.76, 8.21 and 9.28 mg L^{-1}, from the stage 1 to 3, respectively). And the acetate concentrations in effluent presented the same change. The CH_4 production produced mainly in the sludge zone of the reactor R1. But less organic matter was oxidated absolutely in the anode while some acetate was converted into CH_4 and CO_2 on the cathode by the *Methanothrix* (Fig. S11 and S12†) in the reactor R2. The change of acetate concentration was a reaction of COD and the reasons were the same as the COD removal.

3.3 Membrane fouling performance

The membrane fouling performance of the reactors R1, R2, is shown in Fig. 3. The reactor R2 presented a better antifouling ability than that of reactor R1. There was a sudden increase in the TMP at 201 days in the reactor R1 because the HRT was decreased to the initial value by hand. And the TMP evolution stepped up in the reactors. And the average TMP growth rate was 0.00301 bar per day in the reactor R1 while 0.00262 bar per day in the reactor R2. Furthermore, the TMP growth rates in the reactor R2 from stage 1 to 3 were 0.00174, 0.00244 and 1.00093 bar per day, respectively. The membrane fouling rate had increased in terms of accelerating the TMP growth, though the membrane fouling was suppressed by the applied voltage. It might be due to more and more electrogenic microorganisms adsorbed and deposited on the cathode membrane surface, resulting in the pores blocked or reduced. It is different from the result in short-term operation.

The membrane modules were taken out from the reactors and the macroscopic representation was showed in Fig. S5.† Surprisingly, the colour of cake layers on the membrane surface in the reactors R1, R2 were a little dark green and dark, respectively. It is worth noting that the reactors were shaded by a layer of aluminum foil except for some areas fitted with a gas bag and electrodes on the top of the reactor R2. No green algae appeared in the liquor.

The morphological microstructure on the used membrane surface was showed in the Fig. S6.† A lot of pollutants covered heavily the membrane surfaces with the complicated network structure. And the quantity of micron-size pores on the membrane surface in the reactor R2 was relatively more than that in the reactor R1. By magnification observation, some pores on the membrane surface might be caused by biogas bubbles bursting in the cake layer.

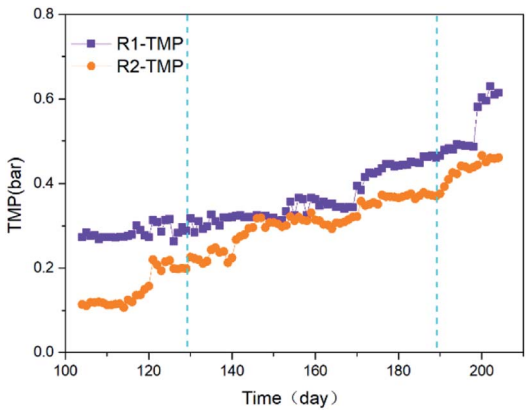

Fig. 3 TMP evolution during the operation of the reactor R1 and R2.

Moreover, the used membranes in the reactors R1, R2, were cut off by the same way. Then the cross-sectional morphologies of the used membranes were taken into scanning electron microscope (SEM) images, as shown in Fig. S7.† The cross-section of a cake layer in the reactor R1 was thick, and prone to being broken easy. In comparison, the cake layer was relatively solid and thin in the reactor R2. These results might be a reaction of different binding force among chemical compositions of cake layers pollutants on the different membrane surfaces. In contrast to the unused membrane surfaces (Fig. S8†), there are less pollutants in the carbon nanotubes mats with negative charges.

3.4 Organic pollutants on the membrane

The Fourier infrared spectrometer (FTIR) spectra showed very similar peaks on the membrane surfaces in the reactors R1, R2. As shown in Fig. 4, there were the same organic groups on the used membrane surfaces, different from those on the unused membrane (HF-PVDF-CNT) surfaces. This is because the FTIR was tested in ATR mode and the depth of measurement was <100 nm. And the depth of pollutant was visible to the naked eye. So the base material had less influence on the FTIR result of the used membrane. For the HF-PVDF-CNT membrane, the strong absorbance appeared at 1546, 1627, 3178 cm^{-1}. They were related with the benzene ring or N–H structure, carbonyl, and the amino groups or carboxyl groups, which proves that the HF-PVDF membrane were modified successfully by carbon nanotubes and dopamine.[26] However, for the used membrane, the strong absorbances at 3200 cm^{-1}, were attributed to the telescopic vibration peak of O–H in the hydroxyl groups, and the C–H telescopic vibration peak was appeared at 2900 cm^{-1}.[29] The materials had strong correlation peaks for absorption, such as 1652 and 1540 cm^{-1}, caused by amide band I and II, respectively. A peak at 1039 cm^{-1} was due to C–O in polysaccharose.[30] Furthermore, the relevant infrared absorption peaks on the membrane surface in the reactor R1 were much stronger than those in the reactor R2. It suggests that more proteins and polysaccharose were adsorbed on the membrane surfaces in the system R1.

EEM fluorescence spectroscopy is showed in the Fig. 5. Overall, there were four mainly strong absorption peak in each spectrum, T_1^1, T_1^2, T_2^1 and T_2^2, respectively. These peaks (T_1^1 and T_1^2) were related to tyrosine proteins and others were related to tryptophan proteins.[31] And locations and intensities of above absorption peaks are showed in Table S5.† It could be seen that contents of tyrosine and tryptophan proteins on the membrane surface were 1.16 and 1.34 times as much as these on the electro-assisted membrane surface, respectively.

Moreover, charged cake layers on the membrane surfaces were characterized by zeta potential, as shown in Table S6.† The average zeta potential was −26.77 (±0.27) mV for the pollutants on the membrane surface in the reactor R1, but −22.47

 © 2021 The Author(s). Published by the Royal Society of Chemistry

Open Access Article. Published on 22 September 2021. Downloaded on 11/11/2025 4:36:28 PM.
This article is licensed under a Creative Commons Attribution-NonCommercial 3.0 Unported Licence.

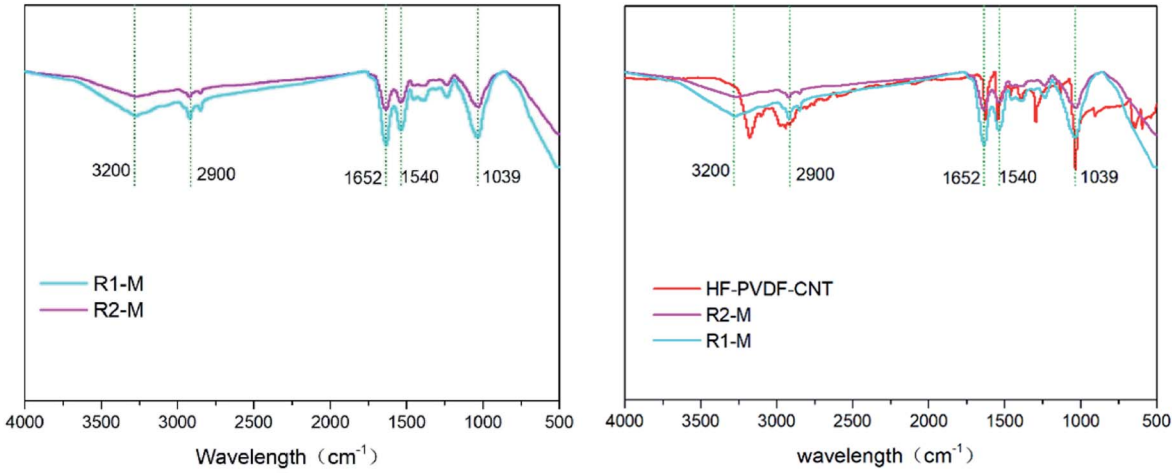

Fig. 4 Infrared spectra of the used membranes in the reactors R1 and R2 (left). Infrared spectra of the unused and used membranes in the reactors R1 and R2 (right).

(±0.27) mV in the reactor R2. The sludge in the reactor R2 contained lower negative charges. It should be taken into consideration that negative surface charges increased linearly with the total extracellular polymer (EPS) content in sludge and increased proteinaceous and carbohydrate fractions played a major role in the EPS.[32] Therefore, the less proteins or EPS with less negative charges deposited and agglomerated on the electro-assisted membrane. These results about EEM fluorescence spectroscopy and zeta potential were corresponding to the above FTIR analysis.

3.5 Salt deposition on the membrane

Besides organic matter, the salt deposition as main inorganic matter was detected by fluorescence spectrometer (XRF), as shown in Table S7.† The same major elements resulted in the membrane fouling of both reactors, including S, Ca, P, Fe, Al, Si, Zn, K, Ni and Cu. In comparison, the content of each element (S, Ca and P) was all >10%. They played an important role in the inorganic salt deposition formation on the membrane surface. In general, the pollutants mainly come from sludge flocs, EPS and sediments in view of source. Surprisingly, the contents of Zn and Cu elements were relatively high and they may come from raw inoculated sludge. In terms of element contents, metal ions in water were deposited mainly on the membrane surface in the form of sulfate, carbonate, phosphate, silicate, hydroxide, oxide. And the main element of positive ion was Ca. These salt depositions were formed into highly viscous gel or dense pollution filter cake layers.[33–35] The content of total elements, including Ca, Fe, Al, Si, Mg and Cu, accounted for 50.34% in the reactor R1, but only 47.09% in the reactor R2. And the proportion of elements, S and P, was 40.56% in the reactor R1, but only 36.73% in the reactor R2. It suggests that a negative cathode potential had a positive effect on pushing the inorganic matter away.

In addition, different sludge particles formed gradually a cake layer with depositing on membrane surface during filtration. The particle size of sludge is showed in Table S8.† Particle size of >90% particles on the electro-assisted

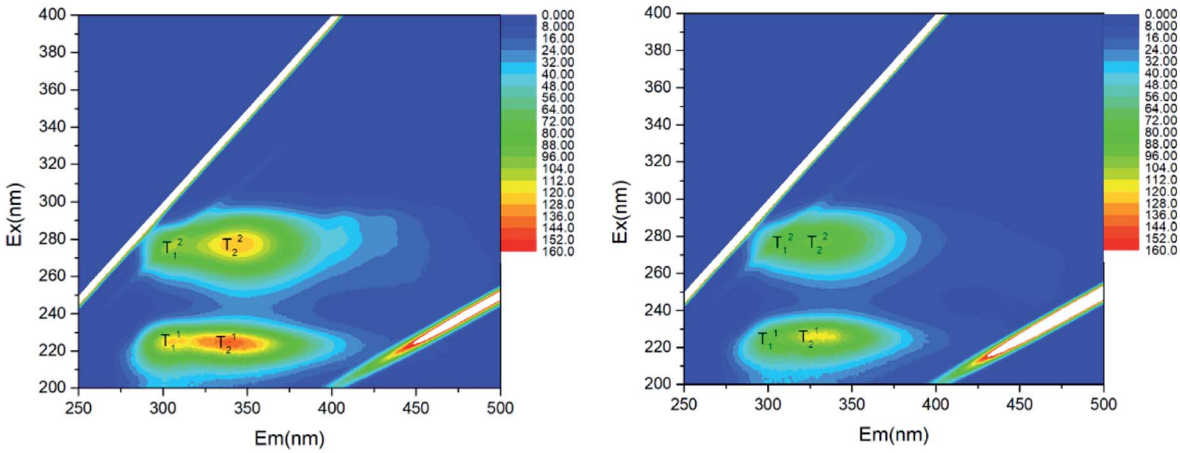

Fig. 5 EEM fluorescence spectroscopy results for the pollutants on the membrane surface in the reactors R1 (left) and R2 (right).

Open Access Article. Published on 22 September 2021. Downloaded on 11/11/2025 4:36:28 PM.
This article is licensed under a Creative Commons Attribution-NonCommercial 3.0 Unported Licence.

membranes was smaller than that on the membrane without applied voltage. And particle size of >50% particles in the anode zone was smaller than that in the sludge zone. These results were opposite to the traditional experimental conclusion about membrane fouling mechanism in the anaerobic membrane reactor. It is normally regarded that small particles were easier than large particles to block the pores on the membrane surface, resulting in increasing density of cake layers and reducing permeability of the membrane in the membrane reactor.[36] Furthermore, the particle size of pollutants on the membrane surface in the reactor R2 was very close to that in the sludge zone of the reactor R1 or R2. And the particle size of pollutants on the membrane surface was the biggest in the reactor R1. The reason might be that, the amounts of microorganisms on the membrane surface in the reactor R2 was more than that in the reactor R1. And there were more abiotic pollutants, including EPS, colloid and salt deposition, on the membrane surface in the reactor R1.

3.6 Electron transfer in the AnEMBR system

The potentials and the current were showed in the Fig. 6. The potential difference was relatively stable in every stage, −0.1 to 0.1 V, −0.7 to −0.8 V and −1.2 to −1.4 V, respectively, from stage 1 to 3. And the current was <0.0001 A, 0.0003 A and 0.0009 A, respectively. Obviously, the total resistance decreased while the potential difference increased. It could be attributed to the change of microbial community through the simulation of the applied voltage as sole environment variable. Hence, it is hypothesized that the increased microbial community (in the anode or cathode zone) had a greater effect on the conductivity of the system, but it might be a reason to increase the TMP growth rate.

3.7 CH_4 production

The Table S9† showed CH_4 production (main biogas, compared with H_2 <5%) during different operation stages. The CH_4 production increased with decrease of the cathode potentials and the largest CH_4 production was 51.85 mL per day, less than that in the reactor R1 (83.45 mL per day). Methane bubbles had a weak effect in the system R2, but electrostatic repulsion had a great positive effect on migrating membrane fouling. It could be attributed to high internal resistance of the membrane module with low transfer efficiency of electrons. So, preparation of the membrane with high conductivity and high membrane flux was an important issue to develop the AnEMBR system. As said Bruce E. Logan, the electrodes with high surface areas and maximize power volumetric densities need to be developed for scaling up and commercialization of microbial electrochemical technology.[37]

In view of CH_4 production, the change of biogas from the system R2 (AnEMBR) was similar to the change of temperature detected by the online monitor. But the biogas production decreased gradually with decreased experimental temperature in the system R1. It is a possible that temperature might seem to have a smaller influence on biogas produced by the system R2 and AnEMBR system seemed to have a potential advantage for the wastewater treatment in the low temperature, for example, in winter.

3.8 Microbial community

The Table S10† showed the microbial alpha diversity in the reactor R1 and R2. The Shannon index and Simpson index were 0.0084 and 5.74, respectively, for the microbial community on the cathode surface in the reactor R2. In comparison, the Shannon index and Simpson index were 0.0063 and 6.00, respectively, for the microbial community on the membrane surface in the reactor R1. These values demonstrated that more species appeared on the membrane surface in the electrochemical environment. In addition, the number of operational taxonomic units (OTU) for the microorganisms on the cathode in the reactor R2 was more than that on the membrane surface in the reactor R1. It shows that more microbes had appeared on the cathode and was far more than that in the reactor R1. Importantly, just to confirm above analysis about membrane fouling performance and mechanism.

Furthermore, the main microbial species and proportions were presented at the class and gene levels on the membrane surface of the reactors R1 and R2, in the Fig. S9–S12,†

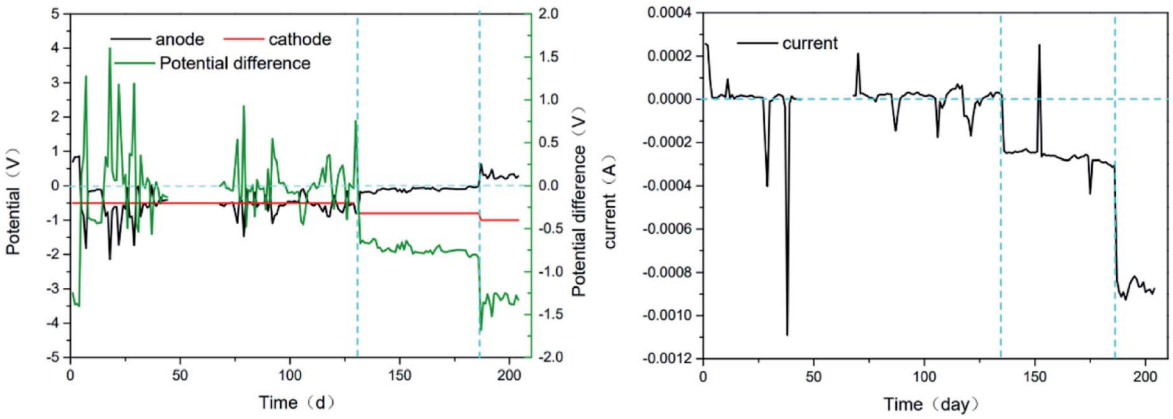

Fig. 6 Potential on anode and cathode and potential difference between anode and cathode (left). The current through the system R2 measured by the electrochemical workstation (right).

 © 2021 The Author(s). Published by the Royal Society of Chemistry

Open Access Article. Published on 22 September 2021. Downloaded on 11/11/2025 4:36:28 PM.
This article is licensed under a Creative Commons Attribution-NonCommercial 3.0 Unported Licence.

respectively. The proportions of *Methanomicrobia* group at the class level were 1.78% and 4.49% of the microbial community on the membrane surface of the reactors R1 and R2, respectively. The result explains the CH_4 production observed in this study. *Anaerolineae* and *Clostridia* groups for degrading soluble organic matter[38,39] on the membrane surface of the reactor R2 (5.17% and 8.14%, respectively) were higher than those of the reactor R1 (7.45% and 2.28%, respectively). And the exoelectrogenic bacteria, mainly including Betaproteobacteria, Deltaproteobacteria and Grammaproteobacteria, on the membrane surface of the reactor R2 accounted for 1.96%, 10.98% and 2%. The values were all more than those of the reactor R1 (0.7%, 9.08% and 0.79%, respectively). Furthermore, an acetoclastic methanogen named *Methanothrix* was the dominant methanogens on the cathode of the reactor R2, accounting for 3.79%. The value was far higher than that on the membrane surface of the reactor R1. *Methanothrix* could participate in direct electron transfer (DET) to produce CH_4 using the CO_2 reduction pathway or acetate decarboxylation pathway.[40] In addition, the genus *Desulfovibrio* was an important and dominant sulfate-reducing bacteria community[41] on the cathode of the reactor R2 (2.39%). In comparison, the proportion of the genus *Desulfovibrio* was only 0.85% on the membrane surface of the reactor R1. Some *Desulfovibrio* species could use directly the electrons and energy from the cathode[42] or hydrogen, organic acids, or alcohol.[43] And H_2 was only utilized when acetate presented.[43] The exoelectrogenic bacteria was beneficial for improving bioelectrochemical methane gas production in the system R2.

4. Conclusions

The amplifying AnEMBR system was operated at different applied voltages for 204 days. The system performance in the long-term operation was different from that in the short-term operation. There were good membrane-antifouling ability and membrane separation contribution in the AnEMBR, compared with AnMBR. But the performance was deteriorated easily in the long-term operation of the AnEMBR system. The number of microorganisms increased highly with stimulation of the applied voltage, which might result in increasing membrane fouling rates in terms of the TMP and reducing the service life of the membrane if the reactor was operated in a long time. The exoelectrogenic bacteria, and methanogens content on the cathode was much higher than the AnMBR, which may be related to the dark cathode surface. As the first study about a long-term operation of amplifying AnEMBR system, the results provide an important theoretical foundation for the further development of AnEMBR technology in the real engineering.

Conflicts of interest

The authors declare no competing financial interest.

Acknowledgements

The authors acknowledge funding support from the National Natural Science Foundation of China (51478015).

References

1 G. Skouteris, D. Hermosilla, P. López, C. Negro and Á. Blanco, *Chem. Eng. J.*, 2012, **198**, 138–148.
2 D. C. Stuckey, *Bioresour. Technol.*, 2012, **122**, 137–148.
3 H. Ozgun, R. K. Dereli, M. E. Ersahin, C. Kinaci, H. Spanjers and J. B. van Lier, *Sep. Purif. Technol.*, 2013, **118**, 89–104.
4 P. Bakonyi, N. Nemestothy, V. Simon and K. Belafi-Bako, *Bioresour. Technol.*, 2014, **156**, 357–363.
5 M. Maaz, M. Yasin, M. Aslam, G. Kumar, A. E. Atabani, M. Idrees, F. Anjum, F. Jamil, R. Ahmad, A. L. Khan, G. Lesage, M. Heran and J. Kim, *Bioresour. Technol.*, 2019, **283**, 358–372.
6 S. Vinardell, S. Astals, M. Peces, M. A. Cardete, I. Fernández, J. Mata-Alvarez and J. Dosta, *Renewable Sustainable Energy Rev.*, 2020, **130**, 109936.
7 J. Zhang, W. L. C. Loong, S. Chou, C. Tang, R. Wang and A. G. Fane, *J. Membr. Sci.*, 2012, **403–404**, 8–14.
8 S. Hube, M. Eskafi, K. F. Hrafnkelsdottir, B. Bjarnadottir, M. A. Bjarnadottir, S. Axelsdottir and B. Wu, *Sci. Total Environ.*, 2020, **710**, 136375.
9 R. Wen, R. Bo, Y. Jin and W. Zhang, *J. Environ. Eng.*, 2021, **147**, 04021041.
10 L. Luo, H. Zhong, Y. Yuan, W. Zhou and C. Zhong, *Environ. Sci.: Water Res. Technol.*, 2021, **7**, 1322–1335.
11 A. C. Society, *Next Generation Biomanufacturing Technologies*, ACS Publications, 2019.
12 Y. Tian, C. Ji, K. Wang and P. Le-Clech, *J. Membr. Sci.*, 2014, **450**, 242–248.
13 B. E. Logan, M. J. Wallack, K.-Y. Kim, W. He, Y. Feng and P. E. Saikaly, *Environ. Sci. Technol. Lett.*, 2015, **2**, 206–214.
14 W. Liu, S. Cheng, L. Yin, Y. Sun and L. Yu, *Electrochim. Acta*, 2018, **261**, 557–564.
15 F. Zhang, Y. Ahn and B. E. Logan, *Bioresour. Technol.*, 2014, **152**, 46–52.
16 J. Ma, Z. Wang, D. Suor, S. Liu, J. Li and Z. Wu, *J. Power Sources*, 2014, **272**, 24–33.
17 J. An, N. Li, L. Wan, L. Zhou, Q. Du, T. Li and X. Wang, *Water Res.*, 2017, **123**, 369–377.
18 W. Yang, V. J. Watson and B. E. Logan, *Environ. Sci. Technol.*, 2016, **50**, 8904–8909.
19 K. P. Katuri, C. M. Werner, R. J. Jimenez-Sandoval, W. Chen, S. Jeon, B. E. Logan, Z. Lai, G. L. Amy and P. E. Saikaly, *Environ. Sci. Technol.*, 2014, **48**, 12833–12841.
20 K. Akamatsu, W. Lu, T. Sugawara and S. Nakao, *Water Res.*, 2010, **44**, 825–830.
21 Y. Yang, S. Qiao, R. Jin, J. Zhou and X. Quan, *Environ. Sci. Technol.*, 2019, **53**, 1014–1021.
22 K. Bani-Melhem and M. Elektorowicz, *Environ. Sci. Technol.*, 2010, **44**, 3298–3304.
23 J. Liu, L. Liu, B. Gao and F. Yang, *J. Membr. Sci.*, 2013, **430**, 196–202.
24 X. Xie, C. Criddle and Y. Cui, *Energy Environ. Sci.*, 2015, **8**, 3418–3441.
25 C. M. Werner, K. P. Katuri, A. R. Hari, W. Chen, Z. Lai, B. E. Logan, G. L. Amy and P. E. Saikaly, *Environ. Sci. Technol.*, 2016, **50**, 4439–4447.

Open Access Article. Published on 22 September 2021. Downloaded on 11/11/2025 4:36:28 PM.
This article is licensed under a Creative Commons Attribution-NonCommercial 3.0 Unported Licence.

26 M. Cao, Y. Zhang, B. Zhang, Z. Liu, X. Ma and C. Chen, *RSC Adv.*, 2020, **10**, 1848–1857.
27 W. E. Federation and American Public Health Association, *Standard Methods for the Examination for Water and Wastewater*, Washington, USA, 2005.
28 E. Lie and T. Welander, *Water Sci. Technol.*, 1994, **30**, 91–100.
29 M. Kumar, S. S. Adham and W. R. Pearce, *Environ. Sci. Technol.*, 2006, **40**, 2037–2044.
30 N. C. Nguyen, S. S. Chen, H. T. Nguyen, H. H. Ngo, W. Guo, C. W. Hao and P. H. Lin, *Sci. Total Environ.*, 2015, **518–519**, 586–594.
31 P. G. Coble, *Mar. Chem.*, 1996, **51**, 325–346.
32 X. S. Jia, H. H. P. Fang and H. Furumai, *Water Sci. Technol.*, 1996, **34**, 309–316.
33 S. Hong and M. Elimelech, *J. Membr. Sci.*, 1997, **132**, 159–181.
34 A. Seidel and M. Elimelech, *J. Membr. Sci.*, 2002, **203**, 245–255.
35 D. Chen, L. Weavers, H. Walker and J. Lenhart, *J. Membr. Sci.*, 2006, **276**, 135–144.
36 A. L. Lim and R. Bai, *J. Membr. Sci.*, 2003, **216**, 279–290.
37 B. E. Logan and K. Rabaey, *Science*, 2012, **337**, 686–690.
38 S. Kato, S. Haruta, Z. J. Cui, M. Ishii, A. Yokota and Y. Igarashi, *Int. J. Syst. Evol. Microbiol.*, 2004, **54**, 2043–2047.
39 T. Yamada, Y. Sekiguchi, S. Hanada, H. Imachi, A. Ohashi, H. Harada and Y. Kamagata, *Int. J. Syst. Evol. Microbiol.*, 2006, **56**, 1331–1340.
40 C. Q. Liu, D. Z. Sun, Z. Q. Zhao, Y. Dang and D. E. Holmes, *Bioresour. Technol.*, 2019, **291**, 9.
41 M. T. Madigan, J. M. Martinko and J. Parker, *Brock biology of microorganisms*, Prentice Hall, Upper Saddle River, NJ, 1997.
42 J. P. Hu, C. P. Zeng, G. L. Liu, Y. B. Lu, R. D. Zhang and H. P. Luo, *Bioresour. Technol.*, 2019, **282**, 425–432.
43 O. Basso, P. Caumette and M. Magot, *Int. J. Syst. Evol. Microbiol.*, 2005, **55**, 101–104.

 © 2021 The Author(s). Published by the Royal Society of Chemistry